AIP | Applied Physics Letters

Optical characterization of band-edge property of In6S7 compound

Ching-Hwa Ho, Yi-Ping Wang, and Ying-Sheng Huang

Citation: Applied Physics Letters **100**, 131905 (2012); doi: 10.1063/1.3698334
View online: http://dx.doi.org/10.1063/1.3698334
View Table of Contents: http://scitation.aip.org/content/aip/journal/apl/100/13?ver=pdfcov
Published by the AIP Publishing

Optical characterization of band-edge property of In_6S_7 compound

Ching-Hwa Ho,[a] Yi-Ping Wang, and Ying-Sheng Huang
Graduate Institute of Applied Science and Technology and Department of Electronic Engineering, National Taiwan University of Science and Technology, 43 Sec. 4, Keelung Rd., Taipei 106, Taiwan

(Received 6 December 2011; accepted 11 March 2012; published online 27 March 2012)

The evaluation of band gap, exciton, and electronic structure of an energy compound is crucial and essential. We report direct optical evidence of band gap, band-edge exciton, and white-light photoelectric conversion for a solar-energy material In_6S_7 herein. The direct gap of In_6S_7 is determined to be 0.93 eV. The value is extremely suitable for absorption of full sunlight spectrum extension to near infrared region. © *2012 American Institute of Physics*. [http://dx.doi.org/10.1063/1.3698334]

Recently, green power and sustainable energy have received considerable attentions in life, where a solar-energy material plays a key role for performing photoelectric conversion from natural and artificial light sources. As a competent solar-energy material, the compound must have a direct band gap to reach high absorption coefficient, an appropriate band gap near ~1 eV for efficient use of sunlight, and a high photoelectric-conversion yield to attain high efficiency.

Indium sulfides belong to nontoxic energy materials which contain a lot of stoichiometries and crystalline phases depending on different growth conditions.[1–3] The generally found stoichiometries and phases of indium sulphides are β-In_2S_3,[4] α-In_2S_3,[5] InS,[6] and In_6S_7.[7] The β-phase In_2S_3 (Ref. 4) (i.e., in tetragonal form) is similar to α-In_2S_3 (in cubic form) excepting that cation vacancies of α-In_2S_3 are disordered in lattice.[5] InS crystallizes in an orthorhombic layer structure[6] and In_6S_7 possesses a monoclinic crystal structure.[3] The advanced way to reach a maximum use of solar spectrum is finding a material with its direct band gap close to 1 eV. For indium sulfides, the band gap of In_2S_3 is 1.935 eV.[8] According to the assessment of its gap value, the usage of In_2S_3 can be a buffer layer (or window layer) consisted in a Cu(In,Ga)Se_2 ($E_g = 1.05$–1.68 eV) solar cell[9] or it can dope with some transition metals (Nb or V) to form intermediate band (IB) for absorption of lower-energy photons below band gap.[5,10] Besides, band gap of layered InS was close to red-light portion of approximate 1.9 eV.[6] The value is still larger than the optimum band gap approaching one electron volt. In_6S_7 is a specific member of general indium sulfides whose band gap below 1 eV. Previous study showed In_6S_7 crystals have a promising photovoltaic property with a thermal band gap around 0.75 eV.[11] Nevertheless, all the previously obtained band gaps ranging from 0.64 to 0.89 eV were almost measured by temperature-dependent electrical measurements (thermal band gap),[12,13] absorption measurements,[14] and photoconductivity measurements.[15] No direct optical evidence verifies its direct band-edge character, and transition energies of In_6S_7 have not yet been determined accurately.

In this letter, In_6S_7 layered crystals have been grown by chemical vapor transport (CVT) method without use of any transport agent. A direct excitonic emission (E_X) has been detected by photoluminescence (PL) at low temperature which verifies direct band-edge character of In_6S_7. The excitonic binding energy of E_X was determined to be ~9.4 meV. The direct gap of In_6S_7 has been determined to be $E_g^d = 0.93$ eV by piezoreflectance (PzR)[16] at 300 K. The gap value of In_6S_7 was also verified by surface photovoltage (SPV) and transmission measurements. Photo-voltage-current (photo V-I) measurements of In_6S_7 were implemented using white light-emitting-diodes array (denoted as white LEDs) and halogen lamp (denoted as halogen lamp) as the white light emulators. The In_6S_7 compound demonstrates a well-behaved photoelectric conversion function under the white lights' illuminations, especially in the near-infrared (NIR) range evident by halogen lamp.

The CVT method was utilized to grow In_6S_7 single crystals without use of any transport agent. The starting materials with intended stoichiometry were put into an evacuated quartz ampoule and sealed in vacuum (~10^{-6} Torr). The growth temperature was set as 750 °C (heating zone) → 690 °C (growth zone) with a gradient of −3 °C/cm.[8] The reaction kept 240 h for producing large single crystals. After the growth, the synthetic In_6S_7 crystals formed essentially shiny-like surface and black color with a maximum size up to $0.7 \times 0.5 \times 0.2$ cm^3. X-ray diffraction measurements confirmed monoclinic phase of the as-grown crystals. The unit-cell parameters were determined to be $a = 9.09$ Å, $b = 3.90$ Å, $c = 17.70$ Å, and $\beta = 108.18°$, respectively. The lattice constants are close to the previously reported data.[17] Energy-dispersion x-ray analysis verified the exact stoichiometric ratio of In and S for the as-grown compound. For optical measurements, PzR experiments were implemented by gluing thin specimen on a lead-zirconate-titanate (PZT) piezoelectric transducer driven by a 200 V_{rms} sinusoidal wave at 200 Hz. The measurement setup of PzR has been described elsewhere.[16] For SPV measurement, the thin sheet-type sample was closely attached on a cooper sample holder by indium or silver paste. A cooper mesh contacts the sample surface with indium. It is the top electrode of In_6S_7. A buffer circuit senses and amplifies the photovoltage response derived from the two electrodes. Photoluminescence measurements were carried out using a charge-coupled device (CCD) spectrometer as the detection unit. A 532-nm laser was used for the pumping light source. For photo V-I experiments, the illuminated power densities of the white LEDs and halogen lamp were adjusted to maintain at ~5 mW/cm^2.

[a]E-mail: chho@mail.ntust.edu.tw. Tel.: +886 2 27303772. Fax: +886 2 27303733.

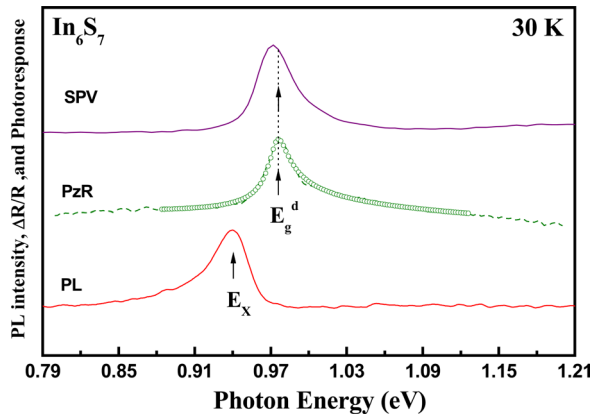

FIG. 1. Experimental SPV, PzR, and PL spectra of In_6S_7 compound at 30 K.

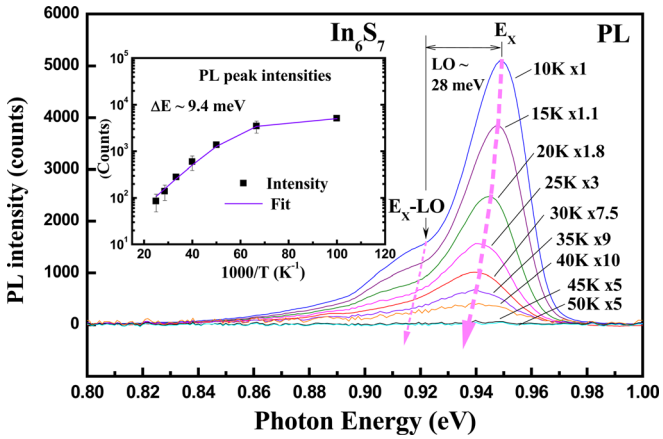

FIG. 2. Temperature-dependent PL spectra of In_6S_7 near band edge from 10 to 50 K. The inset shows PL intensity change of E_X with the increase of temperatures.

The photo V-I measurements were performed via the auxiliary of a semiconductor parameter analyzer.

Fig. 1 shows the SPV, PzR, and PL spectra of In_6S_7 in the energy range between 0.79 and 1.21 eV at 30 K. The dashed line is experimental PzR spectrum, and hollow-circles line is the least-squares fit to a Lorentzian line-shape function appropriate for the interband transition expressed as $\Delta R/R = \mathrm{Re}[\sum A \cdot e^{j\varphi}(E - E_g^d + j\Gamma)^{-m}]$,[18] where A and φ are the amplitude and phase of the line shape, and E_g^d and Γ are the energy and broadening parameter of the interband transition. The value of $m = 0.5$ is used for the first derivative line shape analysis of critical-point transition of direct band gap for In_6S_7.[18] The obtained direct band gap of In_6S_7 (indicated by arrow) is $E_g{}^d = 0.976$ eV at 30 K. The $E_g{}^d$ was also in accordance with the peak photoresponse of SPV spectrum of In_6S_7. In general, the SPV spectrum is approximately proportional to absorption coefficient, which shows step-like photoresponse near band edge. The peak-like SPV feature was also found in the other direct semiconductors such as GaN template and AlInN/AlN/GaN heterostructures.[19] The presence of peak-like SPV is attributed to surface barrier of In_6S_7 is not too high, where a significant recombination flow drives carriers toward surface.[20] Surface recombination is dominant herein. The effect reduces the net excess carriers and decreases the resulting SPV signal for forming a peak photoresponse near band gap. The peak-like SPV feature in Fig. 1 also verifies direct band-gap character of In_6S_7. Another evidence to show direct band-edge nature of In_6S_7 is PL. The PL spectrum in Fig. 1 clearly shows an emission peak denoted as E_X at ~0.942 eV below $E_g{}^d$. This feature is an excitonic emission of In_6S_7 at low temperature.

To evaluate excitonic binding energy of the E_X emission, temperature-dependent PL measurements are carried out and the results are shown in Fig. 2. The E_X feature shows an energy red-shift behavior and an intensity-degradation character with respect to the increase of temperatures from 10 to 40 K. With $T > 45$ K, the PL signal is weakened and not detectable. The energy position of the E_X peak is ~0.948 eV at 10 K, which redshifts to about 0.941 eV at 40 K. The inset in Fig. 2 shows the temperature dependence of PL peak intensities [i.e., I(T)] of E_X. The solid line is a least-squares fit of I(T) to an expression $I(T) = I_0/[1 + C/\exp(\Delta E/kT)]$, where I_0 is the intensity at zero temperature, C is a temperature-independent constant related to capture cross section of the compound, and ΔE is the activation energy. The obtained excitonic binding energy ΔE for E_X is about 9.4 meV. There is also another emission feature denoted as E_X-longitudinal-optical (LO) presented at 0.921 eV at 10 K (see Fig. 2). It is inferred to be a phonon replica of E_X with LO phonon energy of ~28 meV below E_X. The origin of E_X-LO can be identified by parallel temperature dependence of energy shift for both E_X and E_X-LO peaks in Fig. 2. Besides, power-dependent PL measurements at 10 K (not shown here) indicated that the energy separation of LO of the PL peaks remains unchanged under different laser powers' illuminations. It verifies that E_X-LO peak is a phonon-replica emission similar to the other direct semiconductors of ZnO and In_2O_3.[21]

Also shown in Fig. 1, the band gap (E_g) evaluated from PL is $E_g = 0.942\ (E_X) + 0.0094\ (\Delta E) \approx 0.951$ eV at 30 K. The value is still lower than that of $E_g{}^d$ (0.976 eV) in the PzR and SPV spectra by 25 meV. The energy difference between E_g and $E_g{}^d$ is due to exciton-photon interaction that scattered inelastically by phonons (i.e., exciton-ploariton) in the In_6S_7 crystal.[22] When higher-energy photons absorbed by In_6S_7, inelastic scattering event by phonons will eventually render the polaritons exiting the sample with emission in lower-energy photons.

Fig. 3(a) simultaneously shows PzR, transmittance, and SPV spectra of In_6S_7 at room temperature. The transmittance spectrum shows an obvious absorption edge between 0.87 and 1.05 eV. The lower-energy photons of 0.65–0.87 eV may transmit the thin In_6S_7 sample (~80 μm in thickness), while the incident photons higher than 1.05 eV are fully absorbed by the sample. Especially, the center location of the absorption edge in the transmittance spectrum matches well with the peak photoresponse of SPV and the direct gap $E_g{}^d$ by PzR shown in Fig. 3(a). This observation lends apparent evidence that In_6S_7 is a direct semiconductor with direct gap $E_g{}^d = 0.93$ eV at 300 K. The inset in Fig. 3(a) also depicts representative band scheme of In_6S_7 determined by SPV, PzR, and PL measurements. The main part of band edge is essentially dominated by In 5p (E_C) and S 3p (E_V) mixed with small amount of s orbital. The value of $E_g{}^d$ is 0.93 eV and the activation energy of E_X is 9.4 meV. Temperature-dependent PzR spectra of

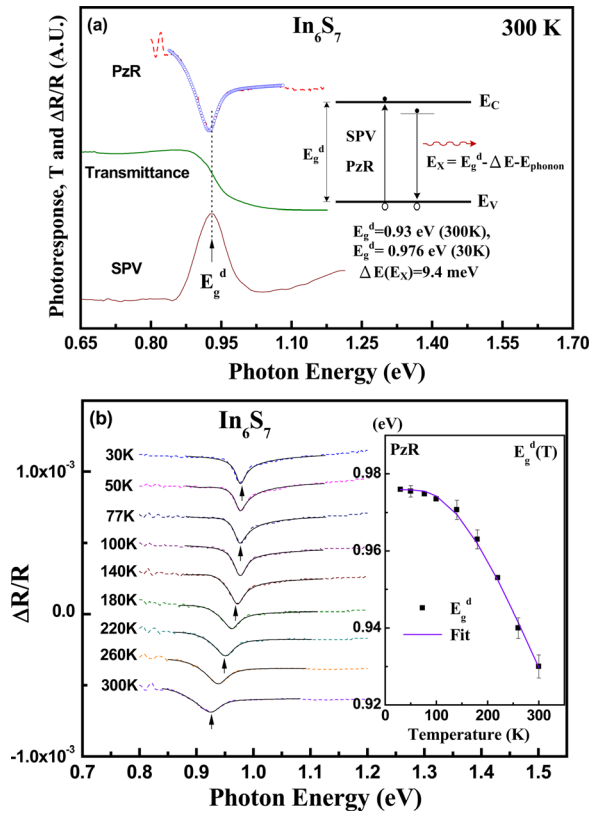

FIG. 3. (a) PzR, transmittance, and SPV spectra of In_6S_7 at 300 K. The representative band scheme is shown. (b) Temperature-dependent PzR spectra and temperature-dependent energy shift of E_g^d for In_6S_7.

In_6S_7 between 30 and 300 K are shown in Fig. 3(b). The dashed lines are the experimental spectra and solid lines are the Lorentzian line-shape fits which yield transition energies indicated with arrows. The E_g^d feature demonstrates an energy red-shift behavior and a line-shape broadened character with the increase of temperatures from 30 to 300 K such as the general semiconductor behaviors. The inset in Fig. 3(b) depicts temperature-dependent energy shift of direct band gap E_g^d for In_6S_7. The solid line is a least-square fit to a Bose-Einstein empirical relationship $E(T) = E_0\text{-}S\cdot\langle\hbar\Omega\rangle\cdot[\coth(\langle\hbar\Omega\rangle/kT)-1]$, where E_0 is the transition energy at 0 K, S is a dimensionless coupling constant related to the strength of electron-phonon interaction, and $\langle\hbar\Omega\rangle$ is the average phonon energy. The obtained values of fitting parameters are $E_0 = 0.976 \pm 0.001$ eV, $S = 4.2 \pm 0.5$, and $\langle\hbar\Omega\rangle = 25 \pm 5$ meV for E_g^d. The average phonon energy $\langle\hbar\Omega\rangle$ is comparable with the phonon energy (i.e., 25 meV) determined by PL and PzR shown in Fig. 1.

In order to evaluate photoelectric conversion behavior of In_6S_7, photo V-I measurements of an In_6S_7 photoconductor (see the measurement setup of Fig. 4) were carried out. Two light sources of one white LEDs and one halogen lamp are, respectively, used. The white LEDs cover a wide spectral range from visible to IR portion with two hump peaks centered at ~450 nm and ~560 nm. The halogen lamp is a broadband blackbody radiation with a main hump peak near ~650 nm which also decreases its intensity toward to the IR range. Two white-light-spot patterns of halogen lamp and white LEDs display different color temperatures as evident in Fig. 4. The color temperature for white LEDs tends to be a

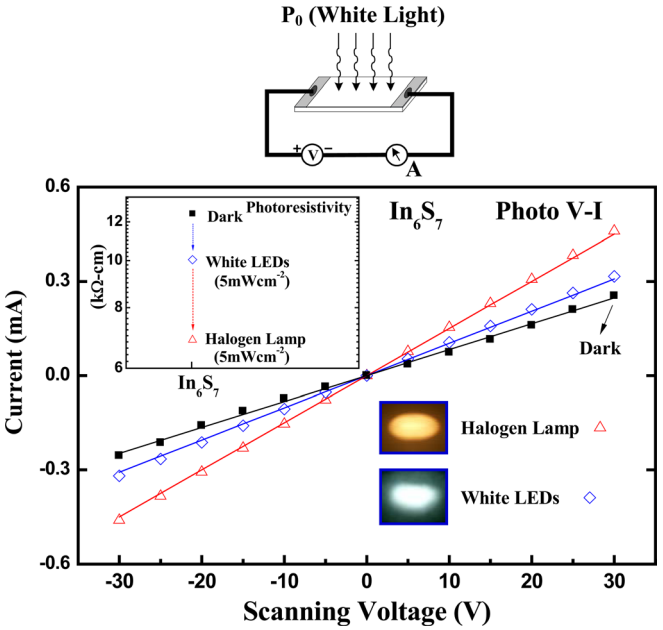

FIG. 4. Photo V-I behaviors of In_6S_7 under different illumination conditions. The photoresistivity change of the compound is shown in the inset.

"cold" light source, whereas the halogen lamp possesses a more "warm" color temperature. The photo V-I curves in Fig. 4 clearly indicate that In_6S_7 shows higher photoelectric conversion yield under the illumination of halogen lamp owing to its lower-band-gap characteristic. The inset in Fig. 4 shows photoresistivities obtained by linear fits of the photo V-I curves under different illumination sources with the same power (5 mW/cm^2). The values of photoresistivities are 12.48 kΩ-cm under dark condition, 10.01 kΩ-cm by the illumination of white LEDs, and 6.85 kΩ-cm obtained by using halogen lamp. The direct gap of In_6S_7 approaches to 1 eV and the near-infrared-portion photons can be efficiently absorbed and converted from the illuminated light sources.

In summary, direct optical gap of In_6S_7 compound is examined. The gap value is evaluated and identified by piezoreflectance, surface photovoltage, and transmission measurements. Photoluminescence measurement reveals one excitonic emission near band edge. This result verifies direct-band-edge character of In_6S_7. The direct band gap of In_6S_7 is determined to be 0.93 eV. The photo V-I measurements show that both near infrared and visible lights can be efficiently absorbed to achieve photoelectric conversion in the In_6S_7 compound.

The authors would like to thank the National Science Council of Taiwan for financially supporting this work under the Project No. NSC97-2221-E-011-164-MY3.

[1]M. F. Stubbs, J. A. Schufle, A. J. Thompson, and J. M. Duncan, J. Am. Chem. Soc. **74**, 1441 (1952).
[2]H. Metzner, M. Brüssler, K.-D. Husemann, and H. J. Lewerenz, Phys. Rev. B **44**, 11614 (1991).
[3]M. Lazell, P. O'Brien, D. J. Otway, and J.-H. Park, J. Chem. Soc. Dalton Trans. **24**, 4479 (2000).
[4]G. A. Horley, P. O'Brien, J.-H. Park, A. J. P. White, and D. J. Williams, J. Mater. Chem. **9**, 1289 (1999).
[5]R. Lucena, I. Aguilera, P. Palacios, P. Wahnón, and J. C. Conesa, Chem. Mater. **20**, 5125 (2008).
[6]T. Nishino and Y. Hamakawa, Jpn. J. Appl. Phys. **16**, 1291 (1977).

[7]H. G. Ansell and R. S. Boorman, J. Electrochem. Soc. **118**, 133 (1971).
[8]C. H. Ho, J. Cryst. Growth **312**, 2718 (2010).
[9]N. Naghavi, S. Spiering, M. Powalla, B. Cavana, and D. Lincot, Prog. Photovoltaics **11**, 437 (2003).
[10]C. H. Ho, J. Mater. Chem. **21**, 10518 (2011).
[11]A. F. Qasrawi and N. M. Gasanly, J. Phys.: Conden. Matter **18**, 4609 (2006).
[12]G. A. Gamal, Semicond. Sci. Technol. **12**, 1106 (1997).
[13]A. F. Qasrawi and N. M. Gasanly, J. Alloys Compd. **426**, 64 (2006).
[14]V. I. Tagirov, I. M. Ismailov, and A. Kh. Khuseĭn, Sov. Phys. Semicond. **12**, 1205 (1978).
[15]N. P. Gavaleshko, M. S. Kitsa, A. Ĭ. Savchuk, and R. N. Simchuk, Sov. Phys. Semicond. **14**, 822 (1980).
[16]C. H. Ho, P. C. Liao, Y. S. Huang, and K. K. Tiong, Phys. Rev. B **55**, 15608 (1997).
[17]J. H. C. Hogg and W. J. Duffin, Acta Crystallogr. **23**, 111 (1967).
[18]D. E. Aspnes, in *Handbook on Semiconductors*, edited by M. Balkanski (North Holland, Amsterdam, 1980), p. 109.
[19]D. Cavalcoli, S. Pandey, B. Fraboni, and A. Cavallini, Appl. Phys. Lett. **98**, 142111 (2011).
[20]L. Kronik and Y. Shapira, Surf. Sci. Rep. **37**, 1 (1999).
[21]C. H. Ho, C. H. Chan, L. C. Tien, and Y. S. Huang, J. Phys. Chem. C **115**, 25088 (2011).
[22]P. Y. Yu and M. Cardona in *Fundamentals of Semiconductors, Physics and Materials Properties*, 3rd ed. (Springer-Verlag, Berlin, 2001).